Available online at www.sciencedirect.com
SCIENCE DIRECT
Catalysis Today 113 (2006) 25–33
CATALYSIS TODAY
www.elsevier.com/locate/cattod

Use of in situ FT-IR and XAS/XRD to study SO_2 poisoning over model Pt/Ba/Al_2O_3 NO_x storage and reduction (NSR) catalysts

James A. Anderson [a,*], Zhaoqiong Liu [a], Marcos Fernández García [b]

[a] *Surface Chemistry and Catalysis Group, Department of Chemistry, King's College, University of Aberdeen, Scotland, Aberdeen AB24 3UE, UK*
[b] *Insituto de Catálisis y Petroleoquímica (CSIC), Campus, UAM, Cantoblanco, 28049 Madrid, Spain*

Available online 20 December 2005

Abstract

Experiments using FT-IR or combined XRD/XAS, both with simultaneous gas phase analysis by MS and chemiluminescence were performed to study reactions over model Pt/Ba/Al_2O_3 NO_x storage and reduction catalysts (NSR). Particular attention was given to the interaction of SO_2 with the catalyst components and how these influenced the NO_x release and reduction stages. Propene was employed as reductant in gas mixtures with/without SO_2. When catalyst was exposed to SO_2 in air, bulk $BaSO_4$ formation occurred readily but without eliminating all of the NO_x storage capacity. When SO_2 was exposed to catalysts in competition with NO_2, no bulk sulphate was detected but a diminished NO_x capacity was measured suggesting the presence of competing adsorbed SO_x species. The latter, in the presence of reductant at higher temperatures, led to rapid displacement of stored NO_x and inhibited carbonate formation.

Keywords: NSR catalysts; NO_x reduction; SO_x poisoning; In situ FT-IR and XAS

1. Introduction

One potential technology to remove NO_x from lean burn gasoline and diesel exhaust streams involve NO_x storage and reduction catalysts (NSR) [1–3]. Storage of NO_x involves an alkaline earth oxide component such as baria, which then releases NO_x either during intermittent engine rich/stoichiometric periods or by injection of hydrocarbon fuel over the catalyst where the released NO_x is then reduced over the noble metal component. The subject has recently been comprehensively reviewed by Epling et al. [4].

The capacity of NSR catalysts to store NO_x is lowered during use due to accumulation of sulphate on the storage component [4–6]. The extent of deactivation may depend upon selection of noble metal/s as there are reports that sulphate formation is promoted by Pt, but inhibited by Rh [7]. Other reports suggest that NO_x storage capacity was lost faster in the presence of SO_2 for a Rh containing catalyst than when Pt alone was employed [8]. The addition of transition metals such as Fe to the Pt/Ba/Al_2O_3 system may enhance durability [9,10] by inhibiting the growth of $BaSO_4$ particles that are formed [10]. Sulphate formation is reduced in the absence of noble metals or in the absence of oxygen [7,11] indicating that the deactivation process involves oxidation of SO_2 to SO_3 over the metal component followed by SO_3 adsorption on the storage component. An alternative to the use of sulphur resistant storage materials using, for example, TiO_2 in place of BaO [12] might involve a selection of metals or combination of metals that exhibit high selectivity for NO oxidation but low selectivity for SO_2 oxidation. In this context, Fridell and co-workers have investigated the addition of metal oxide additives including WO_3, MoO_3, V_2O_5 and Ga_2O_3 on the deactivation of Pt/Ba/Al_2O_3 [13]. Although MoO_3 addition enhanced NO oxidation and showed the lowest SO_2 oxidation activity, the storage capacity of the modified catalyst declined faster than the unmodified Pt/Ba/Al_2O_3. The NO_x storage capacity may be readily regenerated under reducing conditions where the extent of deactivation is relatively low [11,14]. However, in more severe cases, even extended regeneration periods fail to recover the initial storage capacity [5,14]. This degree of difficulty by

* Corresponding author. Tel.: +44 1224 272905; fax: +44 1224 272921.
E-mail address: j.anderson@abdn.ac.uk (J.A. Anderson).

0920-5861/$ – see front matter © 2005 Elsevier B.V. All rights reserved.
doi:10.1016/j.cattod.2005.11.007

which sulphated catalyst is regenerated may be associated with the transition from surface to bulk sulphates [6] or with particle size which governs the ease by which this phase is decomposed [10]. The difficulty in complete regeneration following sulphate poisoning may be linked to the regeneration procedure employed as these invariably involve exposure of the catalyst to a reducing atmosphere at high temperature that leads to the formation of sulphide species. Although some of this sulphide is associated with Ba [5] there is also evidence that sulphide becomes associated with the metallic component [6,15] limiting further regeneration *via* reduction. Pt and Pd both appear susceptible to sulphide formation [6,15], while there is little evidence for sulphidation of Rh. A combination of Pt and Rh was found to provide good sulphur regeneration qualities [8]. For $Pt/Ba/Al_2O_3$ systems, the order of regeneration efficiency was found to be $H_2 > CO > C_3H_6$ [11]. As the presence of water during the regeneration procedure may be beneficial allowing for hydrolysis to remove surface sulphides [11,15] the regenerating gas should contain hydrogen or hydrocarbon. Complete regeneration in hydrogen alone may not be possible, even at elevated temperatures [5] and the addition of CO_2 to a hydrogen containing stream may provide additional benefits when attempting to regenerate sulphate poisoned catalysts as the carbonate is able to displace S^{2-} under rich conditions [5].

While considerable detail regarding these catalysts has been gleaned from these studies, the majority involved conducting the spectroscopic and the reaction studies separately or examined one aspect without the other. Here, we report results obtained using either FT-IR (DRIFT) or combined XRD/XAS with simultaneous gas phase analysis by MS and chemiluminescence for $Pt/Ba/Al_2O_3$ NSR catalysts which had been exposed to SO_2 with particular attention given to the influence which the poison has on each of the components and to distinguish between the extent of formation of bulk and surface species.

2. Experimental

Ten percentage of weight of BaO/Al_2O_3 was prepared by precipitation of $Ba(OH)_2$ from a nitrate solution onto Degussa Aluminoxide C γ-alumina using an ammonia solution. The prepared material was filtered, washed, dried at 363 K (16 h) and calcined in flowing air (100 $cm^3\ min^{-1}$) at 773 K for 2 h. The sample was wet impregnated with 1 wt.% Pt from an H_2PtCl_6 solution. Excess solvent was removed by heating under continuous stirring and the resulting powder dried overnight at 363 K prior to calcination in flowing air (100 $cm^3\ min^{-1}$) at 773 K for 2 h. A BET surface area of 91 $m^2\ g^{-1}$ was measured using Ar as adsorbate on a sample outgassed at 573 K. CO pulse chemisorption on a sample reduced in H_2 at 573 K gave a Pt dispersion of 51.8%. A CO_2:Ba ratio of 0.21:1 was determined from CO_2 adsorption isotherms at 298 K on a sample heated to 1013 K under N_2.

DRIFT spectra were recorded at 4 cm^{-1} resolution as an average of 100 scans using an MCT detector and a DRIFTS attachment (Harrick DRP-series) on a Perkin-Elmer 1750 FT-IR spectrometer. The DRIFTS cell was fitted with CaF_2 windows that gave good resistance to water vapour but limited the lower spectral region to ca. 1100 cm^{-1}. A pc-controlled gas blender manipulated the inlet gas composition, with exit gases from the DRIFTS cell passed to a chemiluminescence (Thermo Environmental Instruments 42C analyser) detector for NO/NO_2/total NO_x analysis and a Baltzer primsa mass spectrometer for other gases. Eighty milligrams of powdered sample was calcined in situ in the DRIFTS cell in dry air (50 $cm^3\ min^{-1}$) at 673 K for 1 h, exposed to 1500 ppm NO_2 for 15 min and cooled to ambient temperature in a NO_2/air flow. The NO_2 was discontinued before a TPD of NO_x from the samples was performed. SO_2 was injected at 673 K as a series of 7 × 1 cm^3 pulses either in flowing air, N_2, or NO_2 in air and then for the former two cases, the catalyst was exposed to NO_2 and then a TPD carried out to determine the storage capacity. In addition to TPD performed in flowing, diluted (7.98%) air in N_2, TPRS were also recorded by heating the sample in a stoichiometric propene (0.355%)/air/balance N_2, 50 $cm^3\ min^{-1}$) between 298 and 873 K at 4 K min^{-1}.

XANES experiments were performed on station 9.3 at Daresbury Laboratories using a double-crystal Si(2 2 0) monochromator with an estimated spectral resolution of ca. 1 eV at an energy of 11.5 keV. Self-supported wafers of the catalysts with a 1.5 absorbance were loaded into an in situ cell, calcined, exposed to NO_2 (with/without SO_2) and heated in a temperature ramp in the presence of a stoichiometric propene/air mixture as described for DRIFTS experiments. XANES spectra at the Pt L_{III} and Ba K edge were obtained in the transmission mode using three ionization chambers with a reference foil between the second and third detectors. XRD patterns were obtained by mounting an INEL position sensitive detector below the in situ XAS cell and collecting counts for 130 s with the monochromator positioned at an energy corresponding to λ = 1.088 Å. The collected data was then calibrated using a pattern collected for a Si wafer under the same conditions. The outlet gases were monitored by use of MS and chemiluminescence as described previously for the DRIFTS measurements.

XAS data was analysed using principal component analysis (PCA) [16,17] which assumes that the absorbance in a set of spectra can be mathematically modelled as a linear sum of individual components, called factors, which correspond to each one of the chemical species present in a sample, plus noise [18]. To determine the number of individual components, an *F*-test of the variance associated with factor *k* and the summed variance associated with the pool of noise factors is performed. A factor is accepted as a ''pure'' species (factor associated with signal and not noise) when the percentage of significance level of the *F*-test, %SL, is lower than a test level set in previous studies at 5% [16,17]. The ratio between the reduced eigenvalues, $R(r)$, (which approaches one for noise factors), are also used in determining the number of factors. Once the number of individual components is set, XANES spectra corresponding to individual chemical species and their concentration profiles are generated by an orthogonal rotation (varimax rotation) which should align factors (as close as

possible) along the unknown concentration profiles, followed by iterative transformation factor analysis (ITFA). ITFA starts with delta function representations of the concentration profiles located at temperatures predicted by the varimax rotation, which are then subjected to refinement by iteration until error in the resulting concentration profiles is lower than the statistical error extracted from the set of raw spectra [16,17].

3. Results and discussion

3.1. Combined FT-IR/TPD

NO_2 was the dominant gas released at 350, 530 and 729 K by fresh, calcined $Pt/Ba/Al_2O_3$ during a TPD in diluted air (Fig. 1a)[11]. NO was released at 352 and at 745 K and represented only 8.5% of the total NO_x released in good agreement with a reported value of 7% [19]. The NO_x storage capacity determined by integration of the TPD profile was 0.475 mmol g^{-1} which equates to a NO_x:Ba ratio of 0.73:1. It is well established that bulk NO_x species are not formed over the alumina support and if it is also accepted that ca. 16% of the alumina surface is covered by nitrate species under these conditions [20], then the corresponding NO_x:Ba molar ratio would be around 0.36:1. This is in good agreement, allowing for the different bulk $Ba(NO_3)_2$ and bulk $Ba(CO_3)$ stoichiometries, with characterization data which gave a CO_2:Ba molar ratio of 0.21:1 under conditions where only surface carbonate was formed [21] and which would indicate that NO_x uptake was also limited to the baria surface. Note that an exact numerical relationship between surface carbonate and nitrate anion: Ba stoichiometry is not expected given the potential to form both 1:1 (monodentate and chelating bidentate) and 1:2 (bridged) type surface species, and most often as a variable proportion of each. However, the absence of in situ XRD evidence for bulk nitrates for samples heated to 873 K and cooled in NO_2 [20,22] would support the claim that only surface nitrates are formed under these conditions.

For catalyst that had been exposed to SO_2 in air at 673 K [11], the TPD profiles (Fig. 1b) were similar to the SO_2-free sample, except that peak intensities were significantly diminished with the exception of the low temperature maxima at 350 K, which was increased for sample exposed to SO_2 in air. The reduced NO_x storage capacity as a consequence of SO_2 exposure to the $Pt/Ba/Al_2O_3$ catalyst (expressed as NO_x released as a % of maximum storage capacity) is summarized in Fig. 2. Storage capacity was reduced to around 30% after exposure to SO_2 in air. Catalysts treated under these conditions gave reflections at 2θ values of 26.0, 28.7 and 42.5° consistent with the expected diffraction pattern of $BaSO_4$ [11]. When the experiment was repeated but exposing the catalyst at 673 K to SO_2 in nitrogen rather than air, no crystalline $BaSO_4$ phase was detected but the NO_x storage capacity was reduced to 36% of its maximum (Fig. 2). The similarity in terms of detrimental effects of SO_2 whether in air or nitrogen irrespective of whether bulk phase sulphate was generated or not, is consistent with the data provided above which indicates that NO_x storage is limited to the surface of exposed baria rather than being the result of bulk nitrate formation and thus surface poisoning alone would be sufficient to reduce the NO_x storage levels. Similarity between the extent to which SO_2 in air or nitrogen affected NO_x storage (Fig. 2) could be reconciled if the retained capacity (ca. 30% in both cases) was due to uptake by the alumina support and that the entire baria surface was poisoned by SO_2 derived species. FT-IR experiments (Figs. 3 and 4) conducted under these conditions (see following paragraph) indicate that this is not the case.

DRIFT spectra obtained after NO_2 exposure to the $Pt/Ba/Al_2O_3$ catalyst are shown in Fig. 3. Bands at 1436 and 1356 cm^{-1} following exposure of the fresh calcined catalyst to NO_2 are consistent with features observed in previous studies irrespective of whether NO or NO_2 was used as a source of NO_x [19–23]. The bands are due to NO_x held as nitrates on baria although as indicated later, a contribution from barium carbonate at ca.

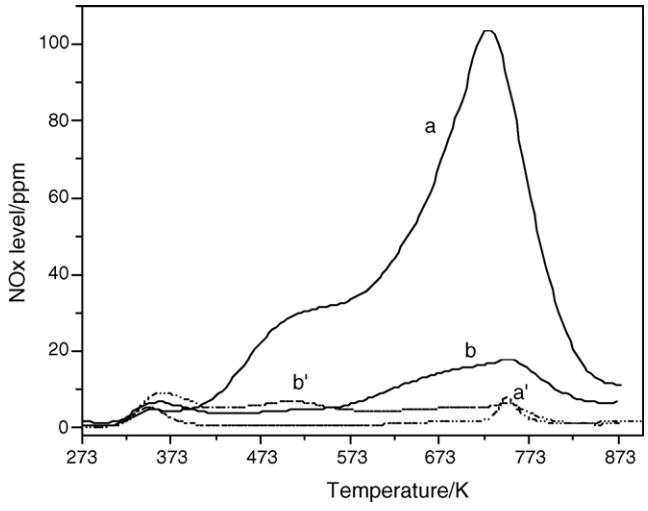

Fig. 1. TPD of NO (dashed line) and NO_2 (solid line) released from $Pt/Ba/Al_2O_3$ on sample (a, a') without SO_2 treatment and (b, b') after SO_2 treatment in air at 673 K and then exposure to 750 ppm NO_2 in N_2/air at 673 K cooling to 298 K, and then heating to 900 K at 4 K min^{-1} in a 7.98% air/balance N_2 gas mixture.

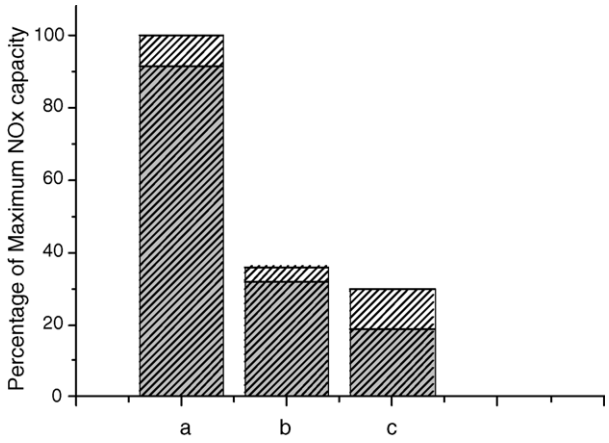

Fig. 2. Relative amounts of NO_x (NO_2 = dark shading, NO = light shading) released from $Pt/Ba/Al_2O_3$ expressed as a percentage of total NO_x released from fresh sample. (a) Calcined sample, (b) calcined sample exposed to SO_2/N_2 at 673 K and (c) calcined sample exposed to SO_2 in air at 673 K.

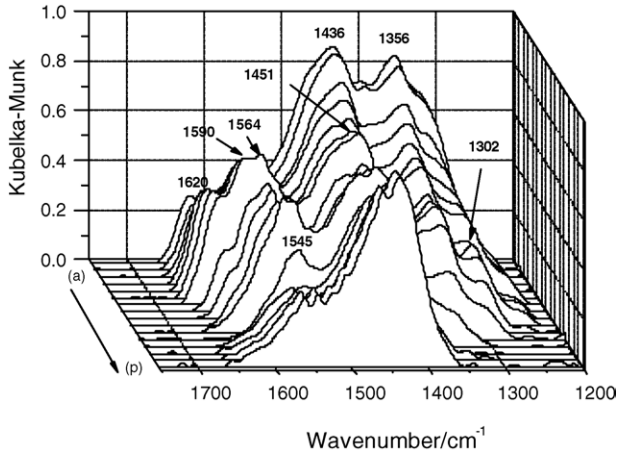

Fig. 3. FT-IR spectra of $Pt/BaO/Al_2O_3$ (a) after NO_2 exposure at 673 K and cooling to RT, with subsequent heating in a stoichiometric propene/air mixture to (b) 298, (c) 335, (d) 377, (e) 411, (f) 444, (g) 478, (h) 511, (I) 556, (j) 601, (k) 648, (l) 692, (m) 727, (n) 783, (o) 821 and (p) 873 K.

1450 cm^{-1} will also contribute to the spectrum. The two features are ascribed to the $\nu_{sym}(NO_2)$ and $\nu_{asy}(NO_2)$ respectively of a monodentate nitrato species. The preferred bidentate adsorption mode of NO_2 on alumina give rise to a higher frequency band, or series of bands due to ν(N=O) [20]. In this study, these nitrates on alumina appeared as a triplet of bands between 1620 and 1560 cm^{-1} [19–23] and were relatively weak in intensity for $Pt/Ba/Al_2O_3$ (Fig. 3a) although these were the more dominant spectral features for the Ba/Al_2O_3 support in the absence of Pt [19]. Although intensities for the two different forms of nitrates are almost certainly not linked to concentration via the same correlation constant, the dominance of the spectrum by features at 1436/1356 cm^{-1} rather than 1620–1560 cm^{-1} would suggest that the majority of stored NO_x was held by the baria rather than the alumina support component. Predominance of similar features for catalysts pretreated at 673 K in either SO_2 in N_2 [11] or SO_2 in air [11] or SO_2/NO_2 in air (Fig. 4a) would suggest that exposed baria sites for NO_x adsorption were still present after SO_2 treatment and that the similarities in the extent to which SO_2 in N_2 or SO_2 in air diminished total NO_x capacity (Fig. 2) was not due to a complete, selective poisoning of the baria and retention of adsorption capacity by the alumina support. Other, alternative explanations for the diminished, but non-zero NO_x capacities of SO_2/N_2 and SO_2/air treated catalysts would include preferential poisoning of baria sites on specific particles (e.g., those in the vicinity of Pt sites) and/or restricted access of NO_x to baria sites that were already populated by adsorbed SO_x.

Fridell [24] distinguished baria sites located close to and further from the active metal in a related context to consider how full NO_x storage could be recovered without complete removal of sulphate species. It was concluded that sulphate generated by removal of S species deposited on the metal function under rich conditions, lead to a poisoning of those baria sites in the vicinity of Pt sites, which were the ones directly responsible for the dynamic NO_x storage (i.e. sites not in the vicinity of Pt might retain SO_x but not influence dynamic storage capacity). In this study, NO_2 rather than NO was chosen to eliminate the need for Pt catalysed formation of the former and in any case, the nitration procedure adopted should occur non-selectively to maximize coverage at all sites unlike the limitations imposed using dynamic, short switch time procedures.

Although nitrate formation from NO_2 may proceed directly over baria without the involvement of Pt [4,25], it is believed that sulphate formation proceeds via SO_2 oxidation to SO_3 [11], a step that required Pt involvement. It could be envisaged that SO_2 in air produces $BaSO_4$ bulk phases, as confirmed by XRD, at sites close to Pt while barium sites in the presence of SO_2/N_2 are randomly populated by some sulphur oxides in some lower oxidation state, such as sulphites or bisulphites [11,26] which permits adsorption of NO_x albeit at diminished concentrations.

To further probe the roles of SO_x on the adsorbed species and on the release and reduction steps, SO_x-free, and SO_2 treated samples were heated in stoichiometric mixtures containing propene and air while simultaneously monitoring the FT-IR spectra of the catalyst (Figs. 3 and 4, respectively) and the evolved NO_x signals (Fig. 5).

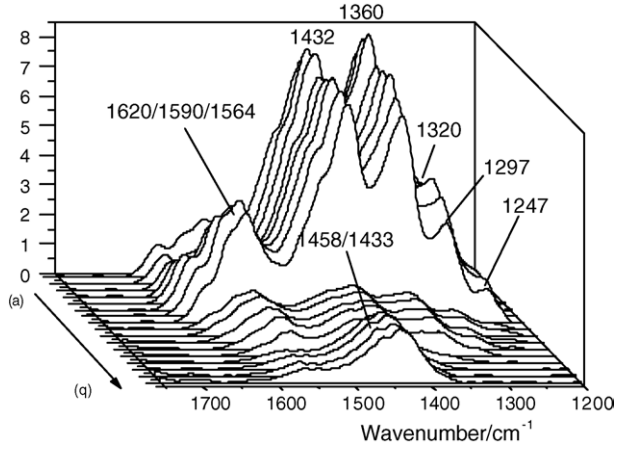

Fig. 4. FT-IR spectra of $Pt/BaO/Al_2O_3$ (a) after NO_2/SO_2 exposure at 673 K and cooling to RT, with subsequent heating in a stoichiometric propene/air mixture to (b) 299, (c) 331, (d) 365, (e) 398, (f) 435, (g) 474, (h) 509, (I) 549, (j) 587, (k) 633, (l) 671, (m) 705, (n) 762, (o) 800, (p) 839 and (q) 873 K.

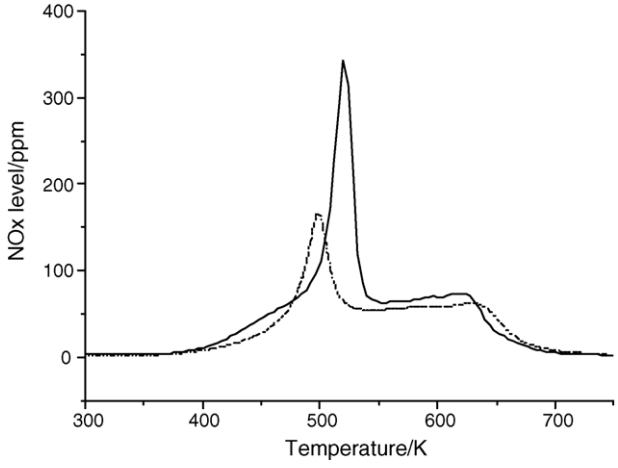

Fig. 5. TPRS of total NO_x released from $Pt/BaO/Al_2O_3$ after NO_2 exposure at 673 K (continuous line) or NO_2 with SO_2 pulsing at 673 K (discontinuous line) followed by cooling to ambient temperature and subsequent heating in a stoichiometric propene/air mixture to 873 K.

Bands due to nitrate on baria (1436/1356 cm^{-1}) progressively lost intensity between 298 and 478 K (Fig. 3b–g) consistent with the gradual increase in released NO_x concentration over this temperature range (Fig. 5). Between 478 and 511 K (Fig. 3g and h) the intensities of all features were more significantly changed and this correlated with the increased rate of NO_x release (Fig. 5), which reached a maximum at 521 K. Although the 1356 cm^{-1} band lost intensity in a gradual manner over the whole temperature range, there was a stepped change in concentration of other adsorbed features (1620–1560 cm^{-1}, nitrates on alumina and 1436 cm^{-1} nitrates on baria) between 648 and 692 K (Fig. 3k and l). At this stage, the mass spec signal indicated that CO_2 formation reached a maximum and the in situ XRD (recorded with the XAS, see later) confirmed that crystalline barium carbonate had been formed. Spectra recorded above 692 K showed progressively smaller contributions due to adsorbed NO_x and over the range 700–873 K, spectra were dominated by a feature at ca. 1450 cm^{-1} (split into components 1461/1439 cm^{-1}) due to barium carbonate [7].

The significant shift in the temperature of the maximum rate of NO_x release from 729 K in air (Fig. 1a) to 521 K in a stoichiometric propene/air mix (Fig. 5) is consistent with previous observations [19–22] and the different possible mechanisms for triggering initial NO release have been discussed in detail [19]. Note that the reductant interaction with the stored nitrate plays a more significant role here than displacement by carbonate resulting from CO_2 formed as a consequence of propene oxidation since a TPD of stored NO_x recorded using 5% CO_2 in air did not result in the same type of profile as that found for the stoichiometric propene/air mixture but showed a gradual increase in NO_x levels with a maximum at 627 K [27]. This would suggest that only the more stable forms of stored nitrate were influenced by the presence of high levels of CO_2.

The evolution of DRIFTS spectra for the SO_2/NO_2 treated catalyst (Fig. 4) followed a similar trend although the maxima at 1432/1360 cm^{-1} were better defined. However rather that the progressive and then stepwise loss of intensity as shown by SO_2-free catalyst, spectra showed a dramatic step loss in intensity between 509 and 549 K (Fig. 4h and i) which corresponded with the maximum rate of NO_x release at ca. 500 K (Fig. 5). Note that the extent to which SO_2 suppressed NO_x capacity, as indicated by the relative integrals of the two plots in Fig. 5, was less than the affect shown in Fig. 1 as the former experiments (Fig. 5) were conducted where SO_2 was competitively adsorbed in the presence of NO_2 rather than being exposed directly to the catalysts in the absence of any other potential competitor (other than traces of CO_2). Bands due to nitrates on both the alumina and baria components were severely suppressed, but still detectable in spectra recorded with the sample above 509 K but these signals effectively disappeared with the sample between 705 and 762 K (Fig. 4m and n) consistent with the NO_x TPD profile dropping to zero in this range (Fig. 5). The spectrum recorded at 762 K showed some growth in the band at ca. 1450 cm^{-1} (split into components 1458/1433 cm^{-1}) due to barium carbonate and these maxima retained intensity in spectra recorded of the sample between 762 and 873 K (Fig. 4n–q). However the relative intensity of the feature due to barium carbonate was very low when compared with the same feature over the ca. 700–873 K range for the SO_2-free reaction (Fig. 3m–p), indicating that the presence of SO_x suppressed the formation of carbonate in this system. Note than unlike experiments conducted where SO_2 was introduced alone, prior to introduction of NO_2 (reported in [11]) no bands indicative of bulk sulphate species were detected which should appear as a rising background below 1300 cm^{-1} [11] due to a band at 1250 cm^{-1} due to formation of bulk barium sulphate [6,24]. Similarly, no surface aluminium sulphate phases were observed as indicated by the absence of a feature at 1386 cm^{-1} [11] and as such would not offer a plausible reason to explain NO_x displacement and negligible carbonate formation at 509 K (Fig. 4h). Note however, that surface sulphate on baria show bands at ca. 1120 and 1060 cm^{-1} [6] which may be formed under these conditions and lead to the spectroscopic changes observed.

3.2. Combined XAS/XRD

The absence of a bulk phase sulphate and the suppression of carbonate formation was confirmed by comparing the in situ XRD patterns for samples exposed to SO_2 in NO_2 at 673 K (Fig. 7) with those treated with only NO_2 (Fig. 6). Expected 2θ values for the different barium compounds using the different radiation sources are listed in Table 1. The samples which had not been exposed to SO_2 showed the growth of a 2θ feature at 16.3° due to barium carbonate (Table 1) with the sample between 630 and 773 K (Fig. 6h–k) which corresponded with conditions for which propene conversion was between ca. 30 and 100% although the 16.3° 2θ feature diminished in intensity above this temperature. The lack of correlation with the carbonate feature in the DRIFTS spectra above 773 K (Fig. 3) would indicate that the latter are due to surface or an amorphous

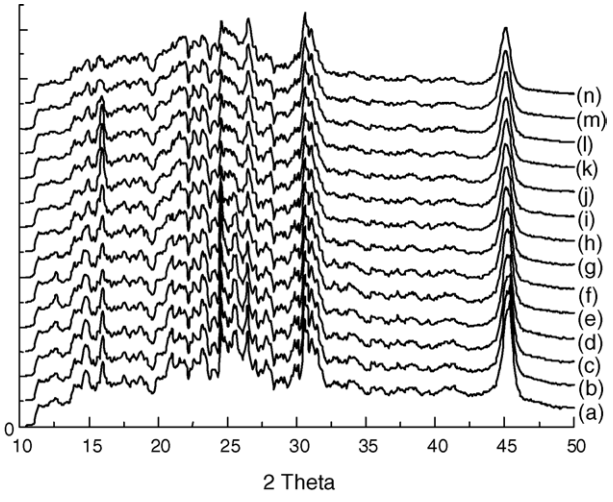

Fig. 6. XRD of $Pt/BaO/Al_2O_3$ (PtL_{III}, $\lambda = 1.088$ Å) after NO_2 exposure at 673 K, then cooling in the same mixture to 298 K then heating in a stoichiometric propene/air mix to (a) 301, (b) 330, (c) 387, (d) 430, (e) 473, (f) 530, (g) 573, (h) 630, (i) 673, (j) 730, (k) 773, (l) 830, (m) 874 and (n) 888 K.

Table 1
Expected 2θ positions using different X-ray sources for relevant barium species

2θ value using λ = 1.542 Å	2θ value using λ = 1.088 Å	Crystalline barium compound
18.8	12.61	Nitrate
21.7	14.56	Nitrate
22.05	14.8	Carbonate
23.65	15.87	Carbonate
24.25	16.27	Carbonate
25.9	17.4	Sulphate
39.5	26.5	Nitrate

type carbonate species which are either more stable than the bulk carbonates or, more likely, are formed as a consequence of bulk carbonate decomposition. Although this feature was also present for the SO_2 treated sample (Fig. 7) no increase was observed, despite achieving 100% conversion of propene to CO_2, but consistent with the DRIFT results (Fig. 4) which showed that carbonate formation was suppressed for catalyst which had been exposed to SO_2 in NO_2 at 673 K. No features due to crystalline $BaSO_4$ phases (Table 1) were detected, again consistent with the absence of a feature at 1250 cm^{-1} in FT-IR spectra indicative of this phase [7].

It is clear that treatment in SO_2 leads to the suppression of adsorbates that are mainly taken up by the baria surface such as NO_2 (Figs. 2 and 5) and also those that are taken up into the bulk such as CO_2 (cf Figs. 3, 4, 6 and 7). Although bulk sulphates are formed under certain conditions [5,6,24], total NO_x capacity is not lost and in fact exposure to the two gases simultaneously leads to a much smaller loss in NO_x capacity (Fig. 5) than when SO_2 is introduced alone (Fig. 2) and no bulk phase sulphate is detected (Figs. 4 and 7). Note that while SO_2 may require oxidation at adjacent Pt sites to facilitate sulphate formation the same is not true for either nitrate from NO_2 or carbonate from CO_2 and so a model involving baria sites which are close to Pt, and readily deactivated due to sulphate formation and those further from Pt which account for NO_x capacity for SO_2 treated catalyst would be consistent with most experimental data. However, it is also clear that bulk sulphate formation is not essential in order to reduce the extent of carbonate formation or the NO_x adsorption capacity.

To obtain further insight into nitrate/sulphate/carbonate formation over Ba, but potentially leading to species lacking long range order which might explain lack of XRD evidence, Ba K-edge XANES measurements were made (Fig. 8) under similar experimental conditions to those used for the FT-IR measurements in Fig. 4. As a consequence of core-hole broadening effects, the Ba K-edge spectra showed no sensitivity to a change in the temperature and/or gas phase composition.

The role of SO_2 in modifying the Pt component was also studied by XANES. There are indications that Pt-sulphide may be formed under certain conditions, for example, when catalyst is exposed to SO_2/propene mixtures at 623 or 773 K [6]. To determine how Pt sites may have been influenced under conditions employed here by the presence of SO_2, experiments were performed at the PtL_{III} edge while exposing the catalyst to NO_2/SO_2 at 673 K and then performing a temperature programme ramp while exposing the catalysts to a stoichiometric propene/air mixture (i.e., same condition as the FT-IR measurements in Fig. 4). Table 1 shows results extracted by employing PCA to the experimental data obtained. In both cases, three species are clearly inferred by the %SL cut-off level of 5% and these each display $R(r)$ values well above 1. However, in the case of the SO_x-free sample (Table 2a), similar statistics for the third and fourth eigenvalue are found while a larger difference is detected between them in the case of the sulphated material (Table 2b). This suggests that four Pt species are present for SO_2 free-samples while only three are present for SO_2 treated Pt. The use of evolving factor analysis [17], a more elaborate statistical test, not shown here for the sake of brevity, supports this conclusion.

XANES spectra of the Pt species detected are presented in Fig. 9A and B with the corresponding concentration profiles along the temperature ramp shown in Fig. 10A and B. Very similar spectra are obtained for species number 1, 2 and 4

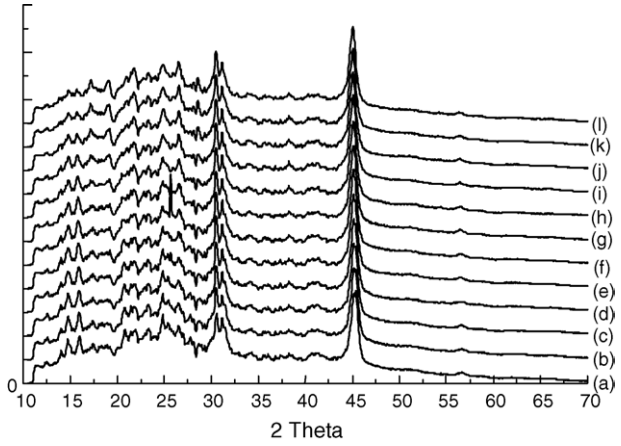

Fig. 7. XRD of Pt/BaO/Al_2O_3 (PtL_{III}, λ = 1.088 Å) after NO_2 and SO_2 exposure at 673 K, then cooling in the same mixture to 298 K with subsequent heating in stoichiometric propene/air mix to (a) 372, (b) 430, (c) 472, (d) 530, (e) 572, (f) 629, (g) 673, (h) 730, (i) 773, (j) 830, (k) 873 and (l) 898 K.

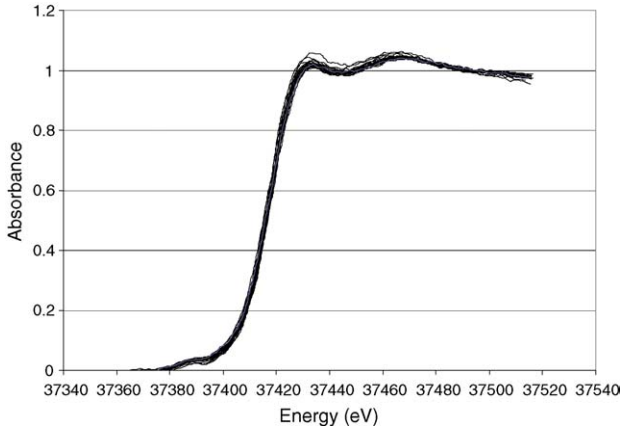

Fig. 8. K-edge XANES spectra recorded for Pt/BaO/Al_2O_3 exposed to NO_2/air at 673 K with SO_2 pulses then cooled to 298 K in NO_2/air and heated in a stoichiometric propene/air mix to 898 K while collecting data.

Table 2
Pt K-edge principal component analysis

Factor	Eigenvalue	% SL	$R(r)$	Variance[a]
a. SO_x-free				
1	883.00	0.00	731.23	99.871
2	1.1328	0.00	214.23	0.028
3	0.00495	2.10	2.56	0.001
4	0.00314	5.18	2.80	
5	0.00083	19.40	1.59	
6	0.00048	29.30	1.16	
7	0.00039	32.70	1.08	
8	0.00033	34.74	0.96	
9	0.00031	34.11	1.06	
10	0.00026	35.98	0.96	
b. SO_2-treated				
1	806.49	0.00	993.27	99.994
2	0.75769	0.00	17.13	0.006
3	0.00411	0.00	24.83	
4	0.00153	5.36	2.99	
5	0.00047	22.87	1.01	
6	0.00043	20.95	1.43	
7	0.00027	28.19	1.10	
8	0.00022	29.93	1.20	
9	0.00017	34.32	0.98	
10	0.00015	34.01	1.11	

Results for SO_x-free and SO_2-treated samples.
[a] Variances less than 10^{-3} are not reported.

(Fig. 9). For both samples, only one oxidized species was detected at the beginning of the ramp. The difference from a typical PtO_2 spectrum, which bears greater similarities [28] with species 3 of Fig. 9A, indicates that Pt(IV) has a modified local coordination with respect to the species in Ref. [28]. This is often a consequence of particle size effects however almost identical (51 cf 51.8%) dispersions would rule out this option here. A more likely option is a modification induced by the presence of N in the first coordination shell. This species will be therefore referred to as Pt^{4+}(N, O). Species 2, an intermediate during the process, is observed; its intermediate white line intensity and edge position indicating a partially reduced oxidation state of Pt, possibly $Pt^{\delta+}$ with δ lying close to 1. A maximum in the concentration of species 2 exists at 575 K, independent of pre-treatment (Fig. 10A). By the end of the temperature ramp, two species, identified as metallic-like Pt(0) (species number 4) and PtO_2-like (species number 3), were present for the SO_x-free sample (Fig. 10A), while the sulphated catalyst still displayed the presence of the intermediate compound $Pt^{\delta+}$ together with the metallic-like Pt(0) species. The lack of evidence for Pt–S [6] would suggest that such species are not formed when oxidants (O_2, NO_x) are present in the gas-phase. Such a conclusion is consistent with a previous report [11] that indicated that the presence of oxygen in the feed stream during rich regeneration periods played an important role in the regeneration period.

Some differences between the catalysts were apparent in the thermal evolution of the concentrations of Pt species (Fig. 10). Below 575 K, Pt^{4+}(N, O) was converted to partially reduced $Pt^{\delta+}$ (species 2) for both samples, however, metallic-like Pt(0) was also present for the sulphated material. The evolution of NO_x loss as illustrated in the TPD profile (Fig. 5) correlates well with the removal of species 1 in the SO_x-free case (Fig. 10A), thus supporting an assignment of species 1 to Pt(IV) associated with adsorbed NO_x. However a shift in the TPD maximum to lower temperatures in the presence of SO_x (Fig. 5) was not reflected in a lowering of the temperature profile of this species (Fig. 10B) suggesting that the initial Pt state was not only influenced by adsorbed NO_x. Sedlmair et al. [6] similarly found using XANES that Pt species were less reducible (in H_2) following exposure to SO_2. Above 575 K, Pt(0) and the PtO_2-like species (No 3) increased in concentration for the SO_x-free catalyst. Between 700 and 800 K their concentrations remained constant, but then responded above 800 K due to the decomposition of PtO_2 to yield Pt(0), a reaction equivalent

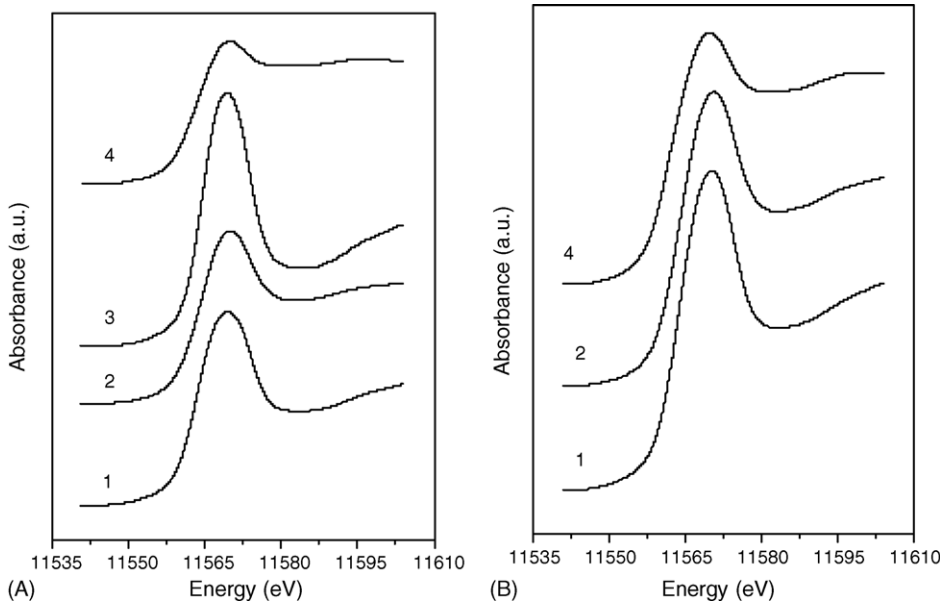

Fig. 9. Predicted pure component XANES spectra for Pt species (A) SO_x-free $Pt/BaO/Al_2O_3$ sample, (B) SO_2-treated $Pt/BaO/Al_2O_3$ sample. See text for details concerning assignment of species.

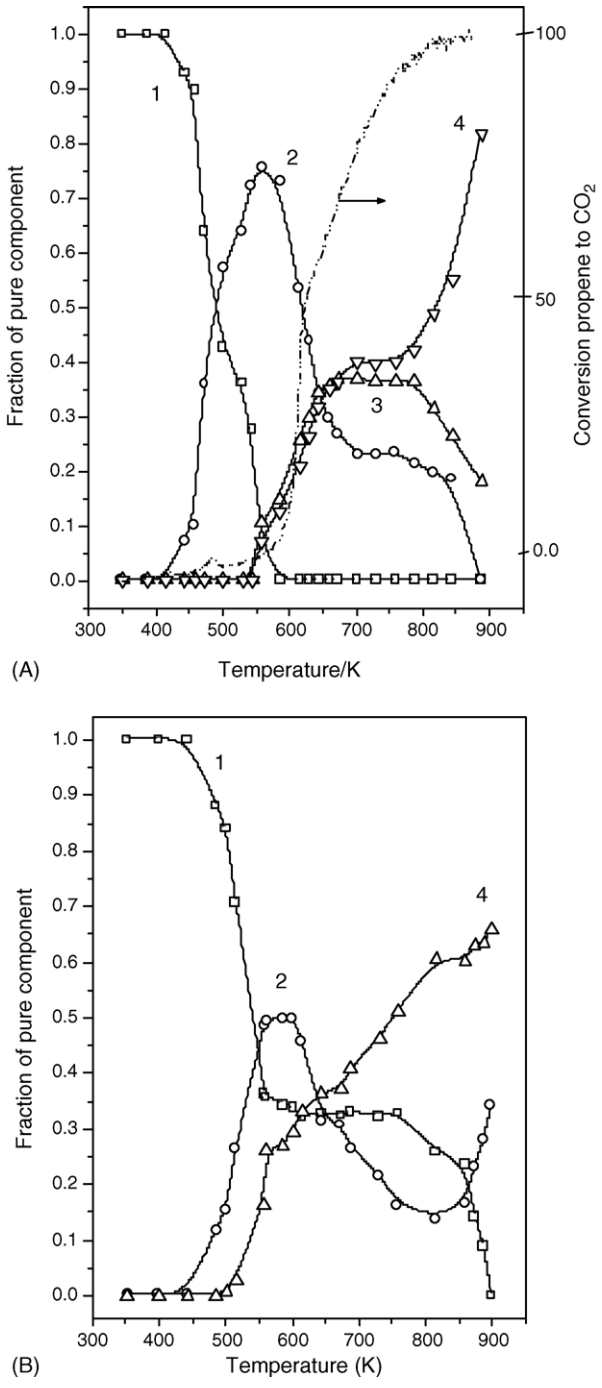

Fig. 10. Concentration profiles along the temperature ramp for the different Pt species presented in Fig. 9 for (A) SO_x-free sample, (B) SO_2-treated sample. Discontinuous line shows conversion of propene to CO_2.

to that observed for the bulk PtO_2 which is expected to decompose to yield Pt metal above 673 K even in an atmosphere of oxygen [29]. For the sulphated catalyst, a continuous decreases in $Pt^{\delta+}$ concentration occurred between 575 and 700 K to yield exclusively Pt(0). Pt^{4+}(N, O) concentration remained constant in this temperature range, consistent with the high levels of gaseous NO_x present over this temperature range, before being transformed into Pt(0) and the intermediate $Pt^{\delta+}$ at above 700 K.

The intersection between complete loss of PtO_2 at ca. 600 K and the onset of Pt(0) formation at ca. 550 K (maximum concentration of species 2; Fig. 10A) for the SO_x-free catalyst marked the light-off of propene oxidation which had reached 100% conversion around 700 K, a temperature which marked the plateau exhibited by both species 3 and 4 (Pt(0)). On this basis, it could be argued that the conversion of species 2 to 3 and 4 was essential for the formation of the active propene oxidation catalyst, with Pt(0) (species 4) being the active phase.

4. Conclusions

Catalysts pretreated in SO_2 show significant, but not total, loss of NO_x storage capacity with barium sulphate being formed if exposure occurs in the presence of air. Bulk sulphate formation is not so readily formed when SO_2 treatment takes place competitively (in the presence of NO_x) although again the result is a suppression of NO_x adsorption. Even when SO_x uptake is restricted to the baria surface, displacement and suppression of carbonate formation occur. Pt–S species are not favored when oxidants are present in the gas stream. Bulk phase Pt reduction takes place before propene activation can occur.

Acknowledgments

We thank Drs. I. Harvey and N. Chinnery for assistance on station 9.3 (SRS Daresbury, UK) and the Royal Society (London) and Cummins Inc., for financial support. Thanks to Dr. W. Epling (Cummins Inc.) for comments on the original manuscript.

References

[1] N. Takahashi, H. Shinjoh, T. Iijima, T. Suzuki, K. Yamazaki, K. Yokota, H. Suzuki, N. Miyoshi, S. Matsumoto, T. Tanizawa, S. Tanaka, T. Tateishi, K. Kashara, Catal. Today 27 (1996) 63.
[2] J.M. Coronado, J.A. Anderson, J. Molec. Catal. 138 (1999) 83.
[3] E. Fridell, M. Skogludh, B. Westerberg, S. Johansson, G. Smedler, J. Catal. 183 (1999) 196.
[4] W.S. Epling, L.E. Campbell, A. Yezerets, N.W. Currier, J.E. Parks II, Catal. Rev. 46 (2004) 163.
[5] S. Pouston, R.R. Rajaram, Catal. Today 81 (2003) 603.
[6] Ch. Sedlmair, K. Seshan, A. Jentys, J.A. Lercher, Catal. Today 75 (2002) 413.
[7] H. Mahzoul, L. Limousy, J.F. Brilhac, P. Gilot, J. Anal. Appl. Pyrol. 56 (2000) 179.
[8] A. Amberntsson, E. Fridell, M. Skogludh, Appl. Catal. 46 (2003) 429.
[9] P.T. Fanson, M.R. Horton, W.N. Delgass, J. Lauterbach, Appl. Catal. B 46 (2003) 393.
[10] K. Yamazaki, T. Suzuki, N. Takahshi, K. Yokota, M. Sugiura, Appl. Catal. B 30 (2001) 459.
[11] Z. Liu, J.A. Anderson, J. Catal. 228 (2004) 243.
[12] H.Y. Huang, R.Q. Long, R.T. Yang, Appl. Catal. B 33 (2001) 127.
[13] J. Dawody, M. Skoglundh, E. Fridell, J. Molec. Catal. A 209 (2004) 215.
[14] C. Courson, A. Khalfi, H. Mahzoul, S. Hodjati, N. Moral, A. Kiennemann, P. Gilot, Catal. Commun. 3 (2002) 471.
[15] L. Limousy, H. Mahzoul, J.F. Brilhac, F. Garin, G. Maire, P. Gilot, Appl. Catal. B 45 (2003) 169.
[16] M. Fernández-García, C. Márquez-Alvarez, G.L. Haller, J. Phys. Chem. 99 (1995) 12565.

[17] C. Márquez-Alvarez, I. Rodríguez-Ramos, A. Guerrero-Ruiz, G.L. Haller, M. Fernández-García, J. Am. Chem Soc. 119 (1997) 2905.
[18] E.R. Malinowsky, Factor Analysis in Chemistry, Wiley, New York, 1991.
[19] Z. Liu, J.A. Anderson, J. Catal. 224 (2004) 18.
[20] J.A. Anderson, B. Bachiller-Baeza, M. Fernández-García, PCCP 5 (2003) 4418.
[21] J.A. Anderson, A.J. Paterson, M. Fernández-García, Stud. Surf. Sci. Catal. 130 (2000) 1331.
[22] J.A. Anderson, M. Fernández-García, Trans. I. Chem. E. 78A (2000) 935.
[23] Ch. Sedlmair, K. Seshan, A. Jentys, J.A. Lercher, J. Catal. 214 (2003) 308.
[24] E. Fridell, M. Skoglundh, SAE paper 2004-01-0080.
[25] I. Nova, L. Castoldi, L. Lietti, E. Tronconi, P. Forzatti, F. Prinetto, G. Ghiotti, J. Catal. 222 (2004) 377.
[26] M. Waqif, P. Bazin, O. Saur, J.C. Lavalley, G. Blanchard, O. Touret, Appl. Catal. B 11 (1997) 193.
[27] Z. Liu, J.A. Anderson, unpublished data.
[28] M. Fernández-García, F.K. Chong, J.A. Anderson, C.H. Rochester, G.L. Haller, J. Catal. 182 (1999) 199.
[29] J.C. Chaston, Plat. Metals Rev. 9 (1965) 51.